ATMOSPHERIC FRAGMENTATION OF THE CANYON DIABLO METEOROID. E. Pierazzo[1] and N. A. Artemieva[2], [1]Planetary Science Institute (1700 E. Ft. Lowell Rd., Suite 106; betty@psi.edu), [2]Institute for Dynamics of Geospheres (Russian Academy of Sciences, Leninsky pr., 38-6, 117334, Moscow, Russia; art@idg.chph.ras.ru).

Introduction: About 50 kyr ago the impact of an iron meteoroid excavated Meteor Crater, Arizona [1], the first terrestrial structure widely recognized as a meteorite impact crater. Recent studies of ballistically dispersed impact melts from Meteor Crater [2] indicate a compositionally unusually heterogeneous impact melt with high SiO_2 and exceptionally high (10 to 25% on average) levels of projectile contamination. These are observations that must be explained by any theoretical modeling of the impact event.

Simple atmospheric entry models for an iron meteorite similar to Canyon Diablo indicate that the surface impact speed should have been around 12 km/s [Melosh, personal comm.], not the 15-20 km/s generally assumed in previous impact models [e.g., 4,5]. This may help explaining the unusual characteristics of the impact melt at Meteor Crater.

We present alternative initial estimates of the motion in the atmosphere of an iron projectile similar to Canyon Diablo, to constraint the initial conditions of the impact event that generated Meteor Crater.

Atmospheric Entry Model: To study the motion of an iron projectile in the Earth's atmosphere we use the model of separated fragments, first suggested in [6] and later developed in [7,8,9]. In contrast to the widely used pancake model [10,11], that treats the disrupted meteoroid as a deformable (but continuous) liquid, this approximation allows us to define a mass-velocity distribution on the surface for the solid fragments that create craters (for high final velocity) or that may be found as meteorites (for low final velocity). The model takes into account successive fragmentation and ablation of individual fragments (where the number of fragments, *n*, is 1 at the beginning, and may be as large as a billion of fragments at the end). The meteoroid is subjected to disruption into a pair of fragments if dynamic loading exceeds its strength, which depends on the projectile type and size. The values for fragment mass and direction of repulsion are randomly defined. Usually fragments have a higher strength than the initial body, but may be disrupted again later into a new pair, and so on. The equation of motion is solved for each individual fragment [12], with an additional equation describing repulsion.

We begin our model with an iron projectile 30 m in diameter ($1.67 \cdot 10^8$ kg) with an initial velocity of 18 km/s, impact angle of 45º, density of 7800 kg/m^3 and ablation coefficient of 0.07 s^2/km^2. The tensile strength of the Sikhote-Aline iron shower is known from the laboratory measurements to be equal to $4.4 \cdot 10^8$ dyn/cm^2 for a 1 kg sample. However, the strength of larger bodies is substantially lower due to the presence of small cracks and faults. Moreover, each fragment may have its own unique strength. For this reason for every new fragment with mass *m* we use random variations of strength, distributed near an average value σ defined by a Weibull statistics: $\sigma = \sigma_0 (m_0/m)^{\alpha}$, where m_0 and σ_0 are the mass and the strength values of the Sikhote-Aline sample, α is a constant in the range 0.1-0.25, depending on the projectile type. The final result, in terms of the size-frequency distribution of the fragments and their velocities, may differ substantially dependintg on a random choice of strength: in some cases a "strong" fragment survives the flight and creates a large crater, while in other occasions there are many smaller fragments which strike the surface with lower velocity, equivalent to a loose projectile.

Results: Figure 1 shows the final velocity versus mass of fragments larger than 10^4 kg. "Red" and "blue" variants represent the case of a "strong" projectile, in which one dominant fragment of mass of 4-6×10^7 kg strikes the surface with final velocity ~16 km/s. In the "black" variant, equivalent to a "weak" projectile, all fragments are smaller than 8×10^6 kg and the final velocity is less than 14 km/s. The smallest fragments decelerate to 4 km/s (without doubts, the disruption produce also smaller fragments down to tiny, cm-sized fragments, which strike the surface with terminal velocity, but we excluded them from our simulations). On average, there is a correlation between final velocity and final fragment mass. However, because of multiple fragmentation some small fragments reach the surface with unusually high velocities, up to 16 km/s. These fragments have separated from larger fragments late with no time for de-

Figure 1: Distribution of final velocity versus mass for fragments larger than 10^4 kg. Variants with one dominant fragment and final velocity of 16 km/s ("strong" projectile) are shown in red and blue. Variants with small fragments and final velocity less than 14 km/s ("weak" projectile) are shown in black.

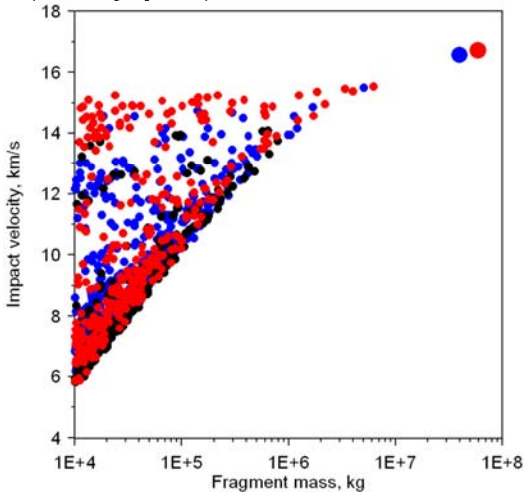

Figure 2: Cumulative number of fragments for the "strong" (red and blue in Fig. 1) and "weak" (black in Fig. 1) projectile cases.

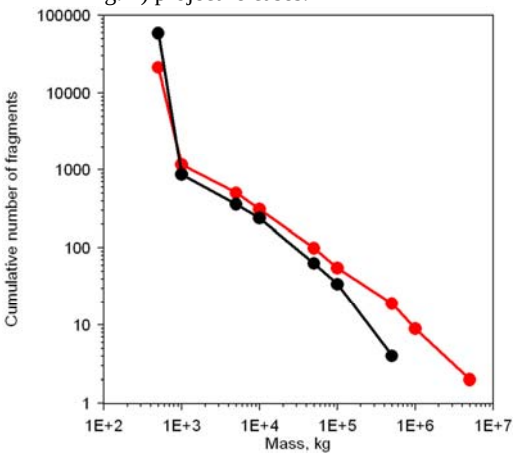

celeration.

Figure 2 shows the cumulative number of fragments for the "strong" and the "weak" projectile cases. In the weak variant the total number of small (500-1000 kg) fragments is 2 times larger (not to mention billions of smaller pieces).

Figure 3 shows the final "strewn field" created by the fragments. In reality this is not a true strewn field, since the fragments separation is smaller than the overlap of the craters formed by their impact. Strewn fields are typical for smaller entry masses; the largest crater in the Earth's strewn field does no exceed 300 m [13]. The variant on the left corresponds to the "strong" variant from Fig.1, on the right – to the "weak" one. The size of the largest crater on the left defined by scaling laws [14] is only a bit less than 1 km and certainly will be even larger because of additional smaller impacts. All crater on the right are less than 300 m, however, their overlap may finally lead to a km-size, but shallow crater, as it was found in the experiments [15]. The dispersion of the craters is of about 400 m in both variants.

Discussion: An accurate inspection of the post-impact crater physical parameters [16] indicates that besides the strong control of the crater shape by regional jointing (its unique "square shape) [17], Meteor Crater is a typical simple crater, with depth/diameter ratio of 0.19 within the statistical range of values listed for bowl shaped lunar craters [18,19].

Thus, we argue that the first scenario - one (or a few) tight largest fragment striking with the velocity of about 16 km/s and a 400m diameter cloud of smaller fragments striking with substantially lower velocity of 6-12 km/s – may agree best with field data.

This work is supported by NASA Grant NAG5-13429.

References: [1] Shoemaker E.M. (1963) in *The Moon, meteorites and comets* (Middlehurst B.M. & Kuiper G.P., Eds), 301-336, Univ. Chicago Press. [2] Hörz F. et al. (2002) *MAPS, 37*, 501. [3] Roddy D.J. et al. (1980) *Proc. LPSC, 11*, 2275. [4] Schnabel C. et al. (1999) *Science, 285*, 85. [5] Passey Q. R. & Melosh H. J. (1980) *Icarus, 42*, 211. [6] Artemieva N. & Shuvalov V. (1996) *Shock waves 5*, 359. [7] Artemieva N. & Shuvalov V. (2001) *JGR 106*, 3297. [8] Bland P. & Artemieva N. (2003) *Nature 424*, 288. [9] Chyba C. F. et al (1993) *Nature, 361*, 40. [10] Hills J.G. & Goda M.P. (1993) *Astron.J 105*, 1114. [11] Melosh J. (1989) *Impact cratering: A geologic process*, Oxford Univ. Press.. [12] Artemieva N. & Bland P. (2003) *LPSC, 34*, Abst. [13] Schmidt R. M. & K. R. Housen (1987) *Int. J Impact Engng* **5,** 543. [14] Schultz P.H. & D.E. Gault (1985) *J. Geophy. Res. 90*, 3701. [15] Roddy D.J. (1978) *Proc. LPSC, 9*, 3891. [16] Shoemaker E.M. (1960) in *Structure of the Earth's crust and deformation of rocks. Rep. 18*, 418, in. Geol. Congr., XXI session, Copenhagen. [17] Pike R.J. (1976) *The Moon, 15*, 463. [18] Pike R.J. (1977) in *Impact and explosion cratering* (Roddy D.J. et al., Eds.), Pergamon Press, 489.

Figure 3: Final. distribution of craters generated by impacting fragments on the surface for two the two main variants ("strong" projectile on the left and "weak" projectile on the right) of figure 2.